6.6

CLIMATOLOGY OF SOIL WETNESS AND TERRESTRIAL WATER STORAGE: COMPARISON BETWEEN MODEL RESULTS AND OBSERVATIONAL DATA

Kooiti Masuda, Jianqing Xu and Ken Motoya
Frontier Research Center for Global Change / JAMSTEC, Yokohama, Japan

1 CONCEPTS

1.1 Introduction

Liquid and solid water on land is one of the important part of the global hydrological cycle as well as of the climate system. Quantitative evaluation of its amount and its rate of change is difficult due to inhomogeneity of land surface and opaqueness of soils for electro-magnetic waves. Global Soil Wetness Project Phase 2 (GSWP2; Dirmeyer et al. 2002) is an attempt to know the behavior of terrestrial water by feeding many land surface models with realistic near-surface meteorological data. Both the models and input data have considerable uncertainties. We need to check the results against more direct observations albeit these are not necessarily more accurate either.

At first we want to discuss the climatological state — the long-term average state and the annual cycle. We choose three variables that can be estimated in continental scale with observational data:

1. terrestrial water storage,
2. diurnal range of surface temperature or that of upward longwave radiation at the surface, and
3. climatological wetness index that can be calculated from surface meteorological data only.

In this report, we introduce the concepts of the three items, and show some results of preliminary analysis comparing the output of a land surface model with observation-based data about the items 1 and 2.

1.2 Terrestrial water storage

What we call 'terrestrial water storage' is a concept based on water balance. It is the mass of liquid plus solid water at and below the surface, including (a) soil water, (b) snowpack (water equivalent), (c) surface water storage in river channels, lakes, reservoirs etc., and (d) groundwater. Note that part of the items (a), (c) and (d) may be frozen, so that ice in permafrost is included in (a) or (d).

Corresponding author address: Kooiti Masuda, Frontier Research Center for Global Change / JAMSTEC, 3173-25 Showa-machi, Kanazawa-ku, Yokohama 236-0001, Japan; e-mail: masuda@jamstec.go.jp

The water balance of a land area (per unit area) can be written as follows:

$$\frac{\mathrm{d}S}{\mathrm{d}t} = (P - E) - R \tag{1}$$

where S is water storage, and P, E, R are precipitation, evaporation, and net runoff, respectively.

Though it is very difficult to know the absolute amount of S which includes the amount of groundwater, we can know the value of S relative to some arbitrary standard level from the balance equation (1), provided that we know $P - E$ and R. We can evaluate R of the catchment of a river gauge station where river discharge is monitored and groundwater discharge can be ignored. We can also estimate $P-E$ from the mass balance of water vapor in the atmospheric column above the area:

$$\frac{\mathrm{d}W}{\mathrm{d}t} = -\mathrm{div}\mathbf{Q} - (P - E), \tag{2}$$

where W is vertically integrated water vapor content (so-called 'precipitable water'), div$\mathbf{Q}$ is horizontal two-dimensional divergence of vertically integrated horizontal transport of water vapor. We can calculate div$\mathbf{Q}$ and W from meteorological data. This approach with operational meteorological data is useful only for the spatial scale of 1000 km or larger, primarily because of the time interval of upper-air soundings (normally 12 hours). Masuda et al. (2001) showed the seasonal cycle of S thus obtained.

It should also be noted that the information about S given by the satellite missions which evaluate the gravity field of the earth (e.g. GRACE) has very similar characteristics to that obtained by the combined land-atmosphere water budget: the relative nature and the spatial scale.

1.3 Diurnal range of surface temperature or of upward longwave radiation at the surface

It is well known that, as long as there is sufficient input of solar radiation, both diurnal range of ground temperature and diurnal range of upward longwave radiation at the surface tend to be larger when the soil is drier. These are often used as indicators of

soil wetness which can be monitored by infra-red remote sensing. These two indicators are almost equivalent because the emissivity of surface materials is not much different from unity in the thermal infrared band of radiation. Why these are related to soil wetness is a simple consequence of surface energy balance. For a crude discussion, we ignore the subsurface heat conduction. Then, large input solar radiation in daytime must be balanced instantaneously by the sum of longwave radiation, latent heat of evaporation, and sensible heat flux. If the ground is moist, latent heat takes large part of it. But if it is dry, only longwave radiation and sensible heat flux are available means of output, both accompany temperature gradient from the surface to the atmosphere. Thus the daytime ground temperature determined by energy balance is higher in the dry condition. For more precise discussions, we need to consider transfer of both energy and water in the soil and in the vegetation canopy. These are tasks of land surface models. The question for the present study is how useful the diurnal range as empirical indicators of soil wetness.

1.4 Potential evaporation and wetness index

Potential evaporation, E_{P}, is defined in the present study (also in Xu and Haginoya, 2001, and Xu et al., 2004), as evaporation expected from a continuously saturated surface. E_{P} thus defined depends on atmospheric conditions (air temperature, air humidity, downward solar radiation, downward longwave radiation, and wind speed) but not on actual surface conditions. Instead we consider an imaginary surface condition with following values of parameters (Kondo and Xu, 1997a, 1997b): a surface roughness of 0.005 m, albedo $ref = 0.06$ (typical of water surface), surface emissivity $\varepsilon = 0.98$, evaporation efficiency $\beta^* = 1$. Surfaces consistent with such parameters include fields with a wet, rough, black surface (i.e., newly ploughed), or a newly planted paddy field with dripping wet leaves.

We consider the daily mean energy balance on such an imaginary surface, and neglect the ground heat flux G. We express turbulent fluxes of sensible and latent heat by bulk transfer formulas. Then we can write:

$$R^{\downarrow} = \varepsilon\sigma T_{\mathsf{SE}}^4 + H + \iota E_{\mathsf{P}} \ , \quad (3)$$

$$H = c_{\mathsf{p}}\rho C_{\mathsf{HU}}(T_{\mathsf{SE}} - T_{\mathsf{AM}}) \ , \quad (4)$$

$$\iota E_P = \iota\rho\beta^* C_{\mathsf{HU}}(q_{\mathsf{SAT}}(T_{\mathsf{SE}}) - q_{\mathsf{AM}}) \ . \quad (5)$$

and

$$R^{\downarrow} = (1 - ref)S^{\downarrow} + \varepsilon L^{\downarrow} \ . \quad (6)$$

$R^{\downarrow}$ is the input radiation at the ground surface. σ is the Stefan-Boltzmann constant (5.670×10^{-8} W m^{-2} K^{-4}), T_{SE} is the calculated surface temperature that satisfies the heat balance equations (3)$-$(6). H is the sensible heat flux, c_p is the specific heat of air, ρ is the air density. T_{AM} is the air temperature, ι is the latent heat of vaporization of unit mass of water, $q_{\mathsf{SAT}}(T_{\mathsf{SE}})$ is the saturation specific humidity at T_{SE}, and q_{AM} is the specific humidity of air.

C_HU is the exchange speed,

$$C_{\mathsf{HU}} = \max(a + b \times 0.7U,\ c \times (T_{\mathsf{SE}} - T_{\mathsf{AM}})^{1/3}) \ . \quad (7)$$

$$a = 0.0027\text{m s}^{-1},\ b = 0.0031,\ c = 0.0036\text{m s}^{-1}\text{K}^{-3}. \quad (8)$$

(The equation (7) was originally developed with the wind speed at 1 m height ($U_{1\mathsf{m}}$). Observations of winds are usually made at 10 m height, and 1-m wind speed is estimated using the logarithmic wind law. Assuming the typical surface roughness 0.005 m, $U_{1\mathsf{m}} \approx 0.7U_{10\mathsf{m}}$.)

The potential evaporation E_{P} can be evaluated from equations (3)$-$(7) as T_{AM}, q_{AM}, $R^{\downarrow}$ and U are given. E_{P} is best estimated with daily meteorological elements, but the quality of calculated results does not suffer if monthly mean elements are used instead, for the reasons outlined in Kondo and Xu (1997b).

The ratio,

$$WI = P/E_{\mathsf{P}}, \quad (9)$$

is defined as a Wetness Index to highlight climatic wetness or dryness. The index relates to the aridity of the climate. By using monthly or annual total values of E_{P}, and precipitation P, climates can be classified into four categories (Kondo and Xu 1997b, Xu 2001, Xu et al.. 2004):

$$WI > 1.0 \ , \text{humid climate}, \quad (10)$$

$$1.0 \geq WI > 0.3 \ , \text{semi}-\text{humid climate}, \quad (11)$$

$$0.3 \geq WI > 0.1 \ , \text{semi}-\text{arid climate}, \quad (12)$$

$$WI \leq 0.1 \ , \text{arid climate}. \quad (13)$$

Various definitions of potential evaporation exist, and many of them (notably those which base on Penman's or Budyko's concepts) take net radiation as a principal element of input. Net radiation includes upward longwave radiation, which is actually determined simultaneously with the surface temperature by the energy balance. It is an advantage of our definition that it does not depends on this. In the context of GSWP2, it is possible to compute potential evaporation from the input data only, and we have made it. Discussion of actual evaporation obtained by land surface models in connection with the potential evaporation will be a subject of our future study.

2 EXPERIMENTATION AND ANALYSIS

2.1 Common framework for analysis

In this presentation, discussion is limited to the climatological annual cycle resolvable by monthly averages. Except otherwise noted, average of the 10-year target period of GSWP2 (1986 – 1995) is considered as the "climatology".

Spatial average values are computed for major river basins of the world. The same 70 Major river basins as in Oki et al. (1995) and Masuda et al. (2001) are considered. The area above river gauge stations where discharge data are available are defined using a 1-degree latitude/longitude version of TRIP.

2.2 Land surface model experiment

We use a land-surface model "MATSIRO" developed by Takata et al. (2003). MATSIRO was developed as a part of CCSR/NIES (Center for Climate System Research of the University of Tokyo and National Institute of Environmental Studies) Atmospheric General Circulation Model. We use a version of MATSIRO developed for CCSR/NIES AGCM Version 5.5b. It includes a big-leaf canopy that can transpire and intercept, 3-layer snowpack, 5-layer soil water with freeze/thaw process, and hillslope hydrology parameterized by a simplified TOPMODEL. To compute river water storage and river discharge, a river routing model "TRIP" (Oki and Sud 1998) is used. Grid-box runoff generated by MATSIRO is fed into TRIP as a one-way process.

Several experiments has been made in conditions mostly similar to the specification of GSWP2 (Dirmeyer et al., 2002). Here we show the results of the experiment that use precipitation input labeled 'GPCC' instead of the GSWP2 standard input. Otherwise the experiment is the same as the GSWP2 standard run ('B0'). The 'GPCC' input precipitation has the same monthly averages as the 'Full Data Product' of Global Precipitation Data Centre (GPCC), and has temporal variation within a month determined by the forecast precipitation of National Centers for Environmental Prediction (NCEP) Reanalysis 2.

In the synthesis of GSWP1 (Oki et al., 2001), it was found that many models underestimate runoff in cold region, and it was suspected that the input rather than the models was biased. It has been known that rain gauges undercatch solid precipitation. Based on intercomparison studies (e.g. Goodison et al., 1998), compensation for the undercatch is incorporated in the production of standard input precipitation data for GSWP2. Examination of the effect of the correction is underway (K. Motoya et al., in preparation), and here we want to avoid complication about the correction.

2.3 Terrestrial water storage

Terrestrial water storage from the model is defined here as the sum of soil water (including frozen part), snow water equivalent and river water storage. In figures (Panel (c) of Figures 1,3,5 and 7), we plot it as bars with colors corresponding to its components: magenta = snowpack; cyan = river water; brown = liquid soil water; yellow = frozen soil water.

"Observed" terrestrial water storage is calculated (K. Masuda et al., in preparation) by basin-atmosphere water balance similar to Masuda et al. (2001). It uses discharge data (Global Runoff Data Centre and others combined) and atmospheric reanalyses (NCEP-NCAR Reanalysis [NCEP1], NCEP Reanalysis 2 [NCEP2] and ECMWF 15-year Re-Analysis [ERA15]). div$\mathbf{Q}$ and W from ERA15 were computed by A. Yatagai (Yatagai and Yasunari, 1998). The period of climatology is 1979−1993 for the analysis involving ERA15, and 1986−1995 otherwise. For river discharge data, we sometimes need to use data of different periods as substitutions. Only the relative value of storage is available from this method. In the figures (Panel (c) of Figures 1,3,5 and 7), we plot the results as curves and the absolute level was so determined the annual minimum value of 'observed' storage matches the 'modeled' one. The colors of the curves correspond to the meteorological data used: red = NCEP1; green = NCEP2; blue = ERA15.

This setting of comparison assumes that the seasonal change of groundwater, more precisely, that of water below 4 m depth (bottom of MATSIRO soil layer in our experiment), can be ignored. This is a compromise and we do not think that this assumption is guaranteed.

2.4 Diurnal range of upward longwave radiation

P. Stackhouse et al. at NASA Langley Research Center have produced the Surface Radiation Budget (SRB) Release 2 data set covering the globe at 1-degree latitude/longitude resolution from July 1983 to October 1995 at 3 hour interval (see `http://srb-swlw.larc.nasa.gov/`). They calculated radiative transfer using the cloud data 'DX' of International Satellite Cloud Climatology Project (ISCCP) and meteorological data of NASA GEOS Reanalysis. There are two versions 'SW' and 'QCSW'

for shortwave and also 'LW' and 'QCLW' for longwave. GSWP2 uses 'SW' and 'QCLW' for its input.

With SRB '3-hourly monthly' averages of 'LW' from November 1985 to October 1995, we calculated climatological monthly diurnal range of upward longwave radiation at the surface. Since it is natural that the range tends to be larger where the average flux is larger, the diurnal range is divided by the monthly average values and shown as non-dimensional 'normalized diurnal range' in the Panel (a) of Figures 1,3,5 and 7.

ISCCP uses geostationary satellites and polar orbiting satellites together. We find that the normalized diurnal range tends to be smaller where observations by geostationary satellites are not available. These areas are covered by multiple polar orbiters, however, and we consider that we can discuss the phase of the seasonal cycle of diurnal range there even though the amplitude of variation is reduced.

We anticipate that the information available by infra-red radiation is related to wetness of in a very shallow part of soil. In our experimentation, the topmost layer of MATSIRO is 5 cm deep. The porosity depends on soil types but generally around 0.4, so it can contain 20 mm of water at most. The water content of the layer ($S_{5\mathrm{cm}}$) is shown in the Panel (b) of Figures 1,3,5 and 7. (MATSIRO has also canopy water storage, but it is not considered here because its capacity is much smaller than the first layer of soil.)

2.5 Water fluxes

To facilitate understanding of water balance, areal mean fluxes of precipitation, evaporation and runoff are shown in Figures 2,4,6 and 8. Bars show the output of MATSIRO in all panels. For precipitation, MATSIRO output just echoes the input and is essentially equal to GPCC Full Data Product. For comparison with other GSWP2 experiments, GSWP2 standard input precipitation is also shown. For evaporation, three curves are shown. These are estimates based on atmospheric water balance using precipitation data of Global Precipitation Climatology Project (GPCP) and $\mathrm{div}\mathbf{Q}$ of reanlyses (red = NCEP1; green = NCEP2; blue = ERA15). The 'runoff' shown here is actually the river discharge divided by the catchment area, for both the model (bars) and observational data (curve).

2.6 Comparison of the annual cycle

To make an objective comparison of the annual cycle, we made harmonic analysis of the annual cycle of S, $S_{5\mathrm{cm}}$, and the normalized diurnal range. The phase of the first annual harmonic is compared. The comparison is considered meaningful where the first harmonic explains more than half of the variance of the 12-month time series and the amplitude is not negligible. (The threshold of amplitude is given subjectively as 10 mm for water storage, 1 mm for soil water in the top layer, and 0.05 for normalized diurnal range.)

3 DISCUSSIONS OF RESULTS

3.1 Terrestrial water storage: Cold region

As examples of cold region, situations of the river basins Lena (eastern Siberia) and Ob (western Siberia) are shown in Figures 1–4. In the cold region, all three reanalyses give similar div$\mathbf{Q}$ and its annual mean value is not much different from annual mean runoff, suggesting that the estimation of terrestrial water storage based on water balance is reliable.

The total storage obtained by MATSIRO also generally agrees with the 'observed' one in both the amplitude and the phase of the annual cycle. In MATSIRO, most of the seasonal change of total storage is contributed by snowpack and river water storage. Seasonal change of total soil water is small, though considerable part of it experience the freeze/thaw cycle. We should examine whether this reflects real behavior of terrestrial water or just peculiarity of MATSIRO.

For the Lena river basin, summer decrease of storage is somewhat slower in the model (Figure 1(c)), which is related to the obvious delay of runoff there (Figure 2(f)). It suggests that the constant river flow speed assumed in our implementation of TRIP is too small for Lena, though it seems to be adequate for other rivers such as Ob and Mackenzie.

3.2 Terrestrial water storage: Tropics

As examples of tropics, situations of the river basins Mekong (Southeast Asia) and Amazon (South America) are shown in Figures 5–8.

In the tropics, div$\mathbf{Q}$ is different from one reanalysis to another. Examining the atmospheric water balance (see curves of evaporation in Figure 6 and 8 (e)), ERA15 and NCEP1 perform much better than NCEP2 for these two basins shown. This evaluation does not apply to all tropical basins, however.

If we choose such reanalysis that produce seemingly realistic div$\mathbf{Q}$, the seasonal cycle of terrestrial water storage obtained with it also generally agrees with the output of MATSIRO. In the humid tropical basins, both soil water and river water contribute to the seasonal variation of total water storage.

3.3 *Diurnal range of upward longwave radiation at surface and soil water in the surface layer*

In some basins such as several ones in China, the annual variability of observed normalized diurnal range is small, despite that the variability of modeled $S_{5\text{cm}}$ is not necessarily small. If the observed variable indicate real soil wetness, it is probable that some process not included in the setting of GSWP, such as irrigation, is important for determining soil wetness in this region. It requires more study to confirm or disprove this idea.

As far as we have non-negligible annual variability of both variables, the variation of the two variables is negatively correlated very well. The phase difference of the annual harmonic between the maximum of $S_{5\text{cm}}$ and the minimum of the normalized diurnal range is always less than (plus or minus) one month.

The relationship between the total storage and the normalized diurnal range is less uniform. The maximum of total storage generally lags behind the minimum of the normalized diurnal range (which is almost synchronous with the maximum of $S_{5\text{cm}}$) by one to three months, but there are a few irregular cases.

Our result about the lag between $S_{5\text{cm}}$ and the total storage broadly agrees with Hirabayashi et al. (2003) who examined the output of a land surface model (JMA-SiB) in the GSWP1 experiment. [Note that the legends for lines in their Fig. 1 were misplaced.] The variables compared in their and our studies are not fully compatible, however. (Their comparison was between $S_{5\text{cm}}$ and the soil water in the root zone.) We should further examine the role of rivers as well as that of soil layers to the lag.

References

Dirmeyer, P., X. Gao and T. Oki, 2002: GSWP-2: The Second Global Soil Wetness Project Science and Implementation Plan. *IGPO Publication Series* No. 37, International GEWEX Project Office (`http://www.gewex.org/`), 65 pp.

Goodison, B., P. Louie and D. Yang, 1998: WMO Solid Precipitation Measurement Intercomparison, Final Report, *WMO/TD*-No. 872, *Instruments and Observing Methods* No. 67, World Meteorological Organization, 88 pp.

Hirabayashi Y., T. Oki, S. Kanae and K. Musiake, 2003: Application of satellite-derived surface soil moisture data to simulating seasonal precipitation by a simple soil moisture transfer method. *J. Hydrometeorol.*, **4**, 929– 943.

Kondo, J, and J. Xu, 1997a: Seasonal variations in the heat and water balances for nonvegetated surfaces. *J. Appl. Meteor.*, **36**, 1676−1695.

Kondo, J, and J. Xu, 1997b: Potential evaporation and climatological wetness index. *Tenki (Bull. Meteorol. Soc. Japan)*, **44**, 875−883, (in Japanese with English summary).

Masuda, K., Y. Hashimoto, H. Matsuyama and T. Oki, 2001: Seasonal cycle of water storage in major river basins of the world. *Geophys. Res. Lett.*, **28**, 3215−3218.

Oki, T., K. Musiake, H. Matsuyama and K. Masuda, 1995: Global atmospheric water balance and runoff from large river basins. *Hydrol. Processes*, **9**, 655−678.

Oki, T. and Y. C. Sud, 1998: Design of Total Runoff Integrating Pathways (TRIP), A global river channel network. *Earth Interactions*, **2**, paper 1. (`http://earthinteractions.org/`).

Oki, T., T. Nishimura and P. Dirmeyer, 1999: Assessment of annual runoff from land surface models using Total Runoff Integrating Pathways (TRIP). *J. Meteorol. Soc. Japan*, **77**, 235−255.

Takata, K., S. Emori and T. Watanabe, 2003: Development of the Minimal Advanced Treatments of Surface Interaction and RunOff, *Global and Planetary Change*, **38**, 209−222.

Xu, J., 2001: An analysis of the climatic changes in eastern Asia using the potential evaporation. *J. Japanese Soc. Hydrol. and Water Resour.*, **14**, 151−170, (in Japanese with English summary).

Xu, J., and S. Haginoya, 2001: An estimation of heat and water balances in the Tibetan Plateau. *J. Meteor. Soc. Japan*, **79**, 485−504.

Xu, J., S. Haginoya, K. Saito, and K. Motoya, 2004: Surface heat balance and pan evaporation trends in Eastern Asia in the period 1971-2000. *Hydrol. Processes*, **18**, in press.

Yatagai, A. and T. Yasunari, 1998:, Variation of summer water vapor transport related to precipitation over and around the arid region in the interior of the Eurasian continent, *J. Meteorol. Soc. Japan*, **76**, 799−815.

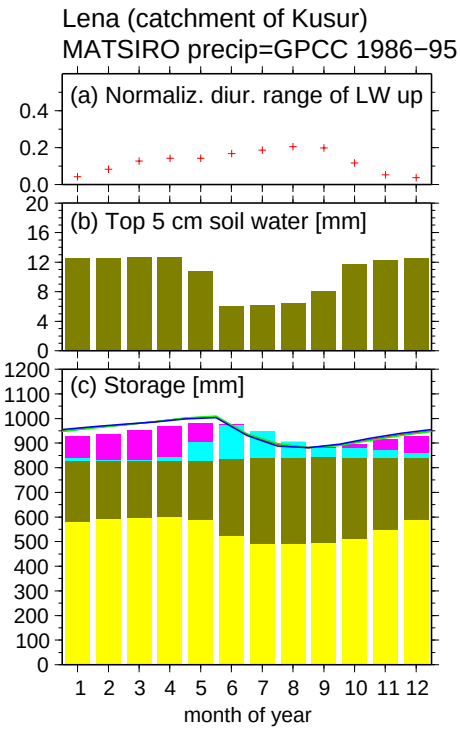

Figure 1: Storage, Lena river basin.

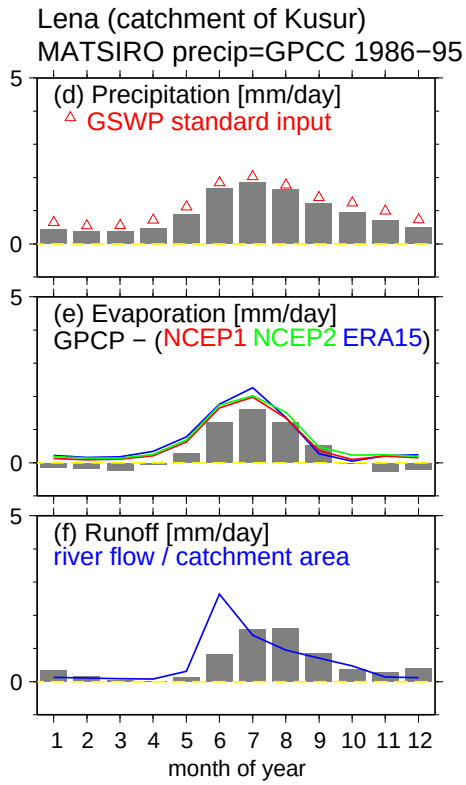

Figure 2: Fluxes, Lena river basin.

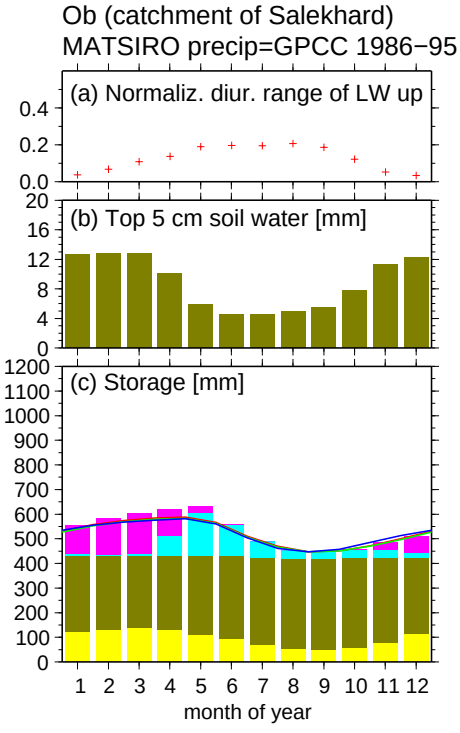

Figure 3: Storage, Ob river basin.

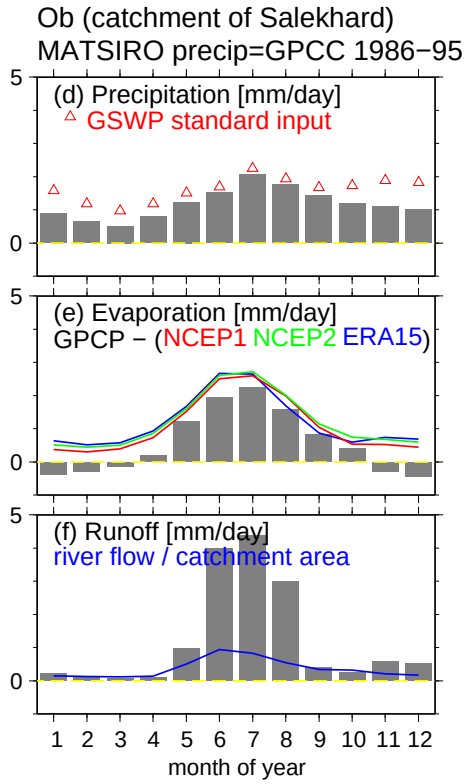

Figure 4: Fluxes, Ob river basin.

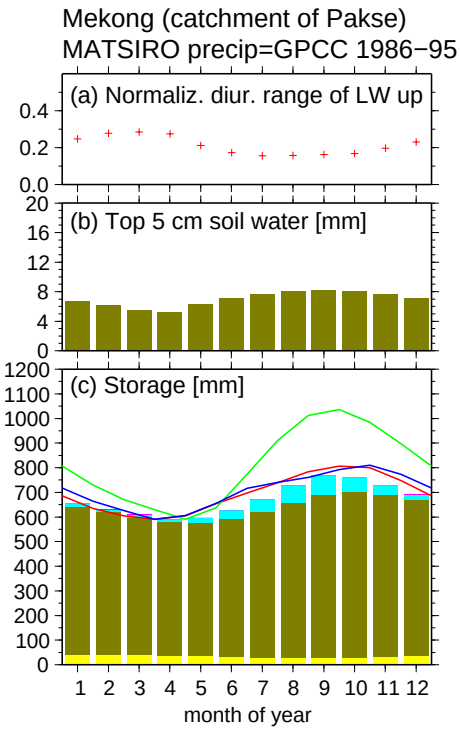

Figure 5: Storage, Mekong river basin.

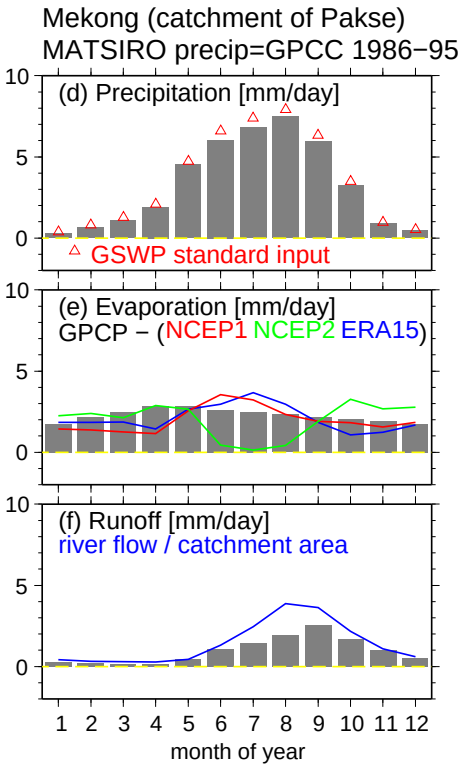

Figure 6: Fluxes, Mekong river basin.

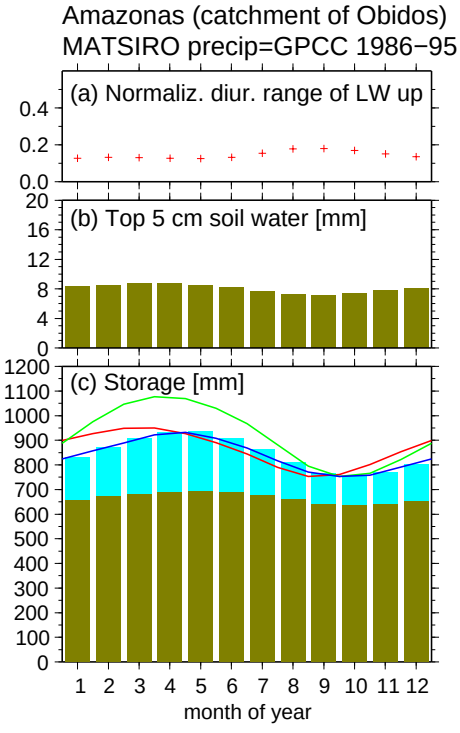

Figure 7: Storage, Amazon river basin.

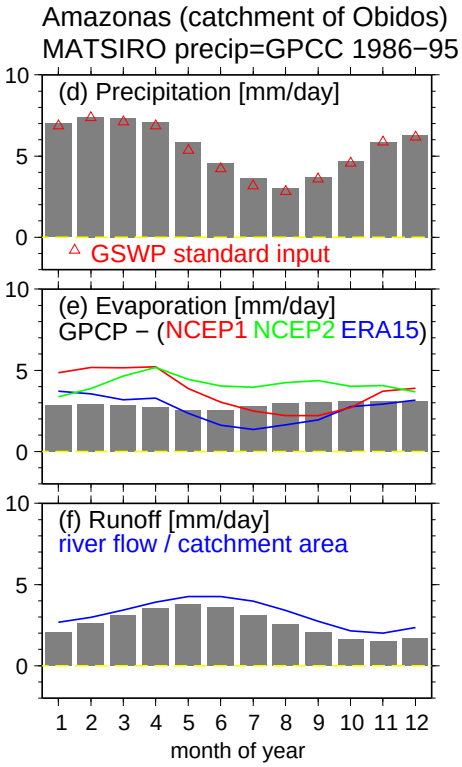

Figure 8: Fluxes, Amazon river basin.